A Model of Erosive Burning of Composite Propellants

Merrill K. King*
Atlantic Research Corporation, Alexandria, Va.

Development of solid rocket motor designs that result in high-velocity flows of product gases across burning propellant surfaces (notably, nozzleless rocket motors) is leading to increased occurrence of erosive burning. In this paper, a physically realistic picture of the effect of such crossflows on composite propellant combustion, based on the bending of columnar diffusion flames by the crossflow, is presented. This bending results in shifting of the diffusion flame heat release zone toward the surface, with consequent increased heat feedback flux from this flame to the surface, and thus increased burning rate. A relatively simple analytical model based on this picture is developed for prediction of propellant burning rate as a function of pressure and crossflow velocity, given only zero-crossflow burning rate versus pressure data. Model predictions and experimental results are compared and reasonably good agreement is found.

Nomenclature

A_2 = constant given by Eq. (16)
A_3, A_4, A_5 = empirical constants relating zero-crossflow burning rate to pressure, obtained by regression analysis of data
AP = ammonium perchlorate
b = pre-exponential in Vielle's burning rate law
c_p = average propellant heat capacity
d_p = oxidizer particle diameter
D = characteristic length for calculation of Reynold's number
f = friction factor
G = crossflow mass flux
k_1, k_2 = constants defined by Eq. (5)
k_3 = erosivity constant in expression of form, $r/r_0 = 1 + k_3 M$
K_1, K_2, K_3 = constants relating standoff distances to pressure and burning mass flux, given by Eqs. (13-15)
$K_1' \ldots K_9'$ = grouped constants defined by Eqs. (25-32)
L_{diff} = diffusion distance (Fig. 1)
L_{kin} = distance associated with oxidizer/fuel reaction subsequent to mixing (Fig. 1)
L_1 = distance associated with oxidizer monopropellant reaction (Fig. 1)
M = crossflow Mach number
MW = molecular weight of propellant product gases
$\dot{m}$ = propellant burning mass flux (linear burning rate × propellant density)
n = exponent in Vielle's burning rate law
P = pressure
$\dot{q}_{\text{feedback}}$ = heat feedback flux from gas flames to propellant surface
Q_{VAP} = heat per unit mass involved in various endothermic processes at or below the propellant surface, e.g., binder pyrolysis or AP sublimation.
Q_{RX} = heat per unit mass involved in various exothermic processes at or below the propellant surface
R = gas law constant
r = linear burning rate
r_0 = linear burning rate at zero crossflow
r_e = erosive contribution to linear burning rate $(r - r_0)$
r_{aft} = linear burning rate at aft end of a grain port
r_{fore} = linear burning rate at fore end of a grain port
Re = Reynolds number
T_{AP} = ammonium perchlorate flame temperature
T_f = propellant flame temperature
T_s = propellant surface temperature
T_0 = propellant bulk temperature
$T_{\text{core gas}}$ = temperature of core gas flowing past a propellant surface.
U^* = friction velocity (shear velocity) of crossflow
$U_{\text{mainstream}}$ = mainstream crossflow velocity
$U_{\text{crossflow}}$ = local crossflow velocity at a given distance from the propellant surface
$V_{\text{transpiration}}$ = blowing velocity of gases produced by propellant combustion normal to the surface, evaluated at the final flame temperature
Y, y = distance from propellant surface
Y^+ = dimensionless distance, $\rho_{\text{gas}} U^* Y / \mu_{\text{gas}}$
γ = specific heat ratio of propellant product gases
λ_A, λ_B = gas thermal conductivity, with an area ratio term for each flame included
ρ_{gas} = propellant product gas density
ρ_s = solid propellant density
θ = angle between propellant surface and vector resultant of crossflow and transpiration velocities (Fig. 1)
τ_1 = characteristic reaction time for AP monopropellant reaction
μ, μ_{gas} = propellant product gas viscosity

Presented as Paper 77-930 at the AIAA/SAE 13th Propulsion Conference, Orlando, Fla., July 11-13, 1977; submitted July 29, 1977; revision received Nov. 16, 1977.

Index categories: Combustion and Combustor Designs; Fuels and Propellants, Properties of.

*Chief Scientist, Research & Technology. Member AIAA.

Introduction

REQUIREMENTS for ever-higher propellant loading fractions in solid-propellant rocket motors and for higher thrust-to-weight ratios have led to development of centrally perforated grain configurations with relatively low port-to-throat area ratios. This, in turn, results in high velocities of propellant gases across burning propellant surfaces in the aft portions of these grains, leading to erosive burning. Moroever, a series of studies has demonstrated that

the nozzleless rocket concept offers significant economic advantages over a more conventional rocket system when considered for some tactical weapon systems. This concept requires that the flow within the bore or central perforation of a grain accelerate to the point at which sonic conditions are achieved at the aft end. In this situation, the high-velocity environment leads to a realm of erosive burning not previously considered. The effects are critical because the erosive burn rate contributions strongly influence performance level, performance repeatability, and thrust misalignment.

In a nozzleless motor, two parameters that affect burning rate, pressure and crossflow velocity, vary strongly from the fore end to the aft end of the grain; namely, static pressure decreases and crossflow velocity increases with distance from the head end of the grain. Assuming that an erosive burning rate expression of the form, $r/r_0 = 1 + k_3 M$ is applicable (with $r_0 = bp^n$), it may be shown[1] that, for constant port area along the grain,

$$r_{aft}/r_{fore} = (k_3 + 1)/(\gamma + 1)^n \quad (1)$$

Values of $(r_{aft}/r_{fore})_{initial}$ as a function of the erosivity constant (k_3) and the burning rate exponent (n) are presented in Table 1 for $\gamma = 1.25$. As may be seen, for the case of no erosion $(k_3 = 0)$ the aft end will recede more slowly than the fore end, due to lower pressure at the aft end. As k_3 increases, the r_{aft}/r_{fore} ratio also increases, going through unity (generally desirable) at a value of k_3 which depends on the burning rate exponent. The results of Table 1 give some indication of the sensitivity of nozzess motor design to the erosive burning characteristics of the propellant and thus point out the importance of information regarding the propellant's erosive burning characteristics to the designer.

Development of a better understanding of the effects of crossflows on solid-propellant combustion would permit the motor designer to either design his grains to compensate for mean erosive burning effects on grain burn pattern, or, knowing how propellant formulation parameters affect erosion sensitivity, vary propellant parameters in such a way as to optimize these effects.

General observations of importance from past experimental studies[2-11] include:

1) Plots of burning rate versus gas velocity or mass flux at constant pressure are usually not fitted best by a straight line.

2) Threshold velocities and "negative" erosion rates are often observed.

3) Slower burning propellants are more strongly affected by crossflows than higher burning rate formulations.

4) At high pressure, the burning rate under erosive conditions tends to approach the same value for all propellants (at the same flow velocity) regardless of the burning rate of the propellants at zero crossflow.

Table 1 Ballistic analysis of a nozzleless motor with uniform port area

$r/r_0 = 1 + k_3 M$, $r_0 = bp^n$

n	k_3	r_{aft}/r_{fore}
0.4	0	0.72
	0.5	1.08
	1.0	1.45
	1.5	1.80
0.6	0	0.61
	0.5	0.92
	1.0	1.23
	1.5	1.54
0.8	0	0.52
	0.5	0.78
	1.0	1.05
	1.5	1.31

5) Erosive burning rates do not depend upon gas temperature of the crossflow (determined from tests in which various "driver propellants" products are flowed across a given test propellant).

There is, however, very little data available for high crossflow velocities (greater than $M \approx 0.3$). In addition, there has been no study in which various propellant parameters have been systematically varied one at a time. Such a study is necessary for determination of erosive burning mechanisms and proper modeling of the erosive burning phenomena.

From the above discussion, it is apparent that development of an analytical model of erosive burning, properly describing the physical effects that result in augmentation of solid composite propellant burning rate by crossflows, coupled with an experimental effort to systematically define the effects of various formulation parameters on erosive burning at crossflow velocities up to Mach 1 is of great importance to the design and development of advanced solid rocket systems.

Background: Existing Models

The objectives of a theoretical model of erosive burning are to provide a means of predicting the sensitivity of propellant combustion rate to gas flow parallel to the ablating surface and to indicate what effect various formulation parameters have on this sensitivity. An acceptable model must account for 1) any effects observed when crossflow gas temperature is varied, 2) observed pressure dependency, and 3) nullification of catalyst activity under erosive conditions. This model should provide an explanation of the observed behavior in terms of the hydrodynamic conditions induced by a crossflow coupled with the chemical and physical processes that constitute the propellant deflagration mechanism.

Over the years, a large number of erosive burning models, of varying degrees of sophistication, have been developed: a list of models examined by this author is presented as Table 2. These models generally fall into one of three categories, as indicated. The first category is based on the assumption that

Table 2 General types of models of erosive burning developed to date

1) Models based on heat transfer from a "core gas" in the presence of cross flow:
- Lenoir and Robillard[12]
- Burick and Osborn[13]
- Zucrow, Osborn, and Murphy[14]
- Saderholm[3]
- Marklund[8]
- Jojic and Blagojevic[15]

2) Models based on alteration of transport properties in region from surface to flame zone by crossflow, generally due to turbulence effects. Includes effects on conductivity from flame zone back to propellant and effects on time for consumption of fuel pockets leaving surface:
- Saderholm et al.[16]
- Lengelle[17]
- Corner (double-base)[18]
- Vandenkerckhove (double-base)[19]
- Zeldovich (double-base)[20]
- Vilyunov (double-base)[11]
- Geckler[21]

3) Models based on chemically reacting boundary-layer theory (homogeneous systems only):
- Tsuji[22]
- Beddini et al.[23]
- Kuo et al.[24]

4) Other:
- Klimov[25]
- Molnar[26]
- Miller[27]
- King

the erosive burning is driven by increased heat transfer from the mainstream gas flow associated with increased heat transfer coefficient with increased mass flux parallel to the grain surface. The best-known and most widely used erosive burning model, that of Lenoir and Robillard,[12] falls into this category. In this model, the authors calculate the total burning rate (r) as the sum of the normal (no crossflow) burning rate and a second erosive term resulting from heat transfer from the "core" flow to the propellant surface. This equation entails an a priori assumption that the pressure-dependent "base" rate (r_0) is unaffected by an increase in total rate at a given pressure, a very unlikely condition within the constraints of other assumptions in the model. This problem has been discussed in detail by King,[28] with derivation of a modified Lenoir and Robillard expression allowing for a coupling of flame standoff distance with burning rate. While Lenoir and Robillard assume $r=r_0+r_e$, allowance for this coupling results in $r=(r_0^2/r)+r_e$. In physical terms, Lenoir and Robillard have failed to account for the fact that increased burning rate, caused by erosive feedback at constant pressure, results in the propellant flame being pushed further from the surface, decreasing its heat feedback rate, and thus decreasing the propellant burning rate part of the way back toward the base rate.

A more general weakness of models in the first category is that these models predict substantial dependence on the temperature of the core gas; such dependence was found by Marklund and Lake[8] to be completely absent. Analysis of the Lenoir and Robillard treatment indicates that the erosive contribution to burning rate (r_e) is given by

$$r_e \propto G^{0.8} \mu_{\text{gas}}^{0.2} (T_{\text{core gas}} - T_s) \tag{2}$$

for a given test propellant and geometry. But, at fixed crossflow velocity and pressure, G is inversely proportional to the core gas (driver propellant products) temperature while μ_{gas} is roughly directly proportional to this temperature. Therefore,

$$r_e \propto T_{\text{core gas}}^{-0.6} (T_{\text{core, gas}} - T_s) \tag{3}$$

However, Marklund and Lake performed a set of experiments in which crossflow velocity and pressure were held constant while the driver propellant was changed from a 1700 K propellant to a 2500 K propellant, with T_s being approximately 800 K in both cases. Thus, the Lenoir and Robillard theory would indicate that

$$\frac{r_{e,2500\,K\text{ driver}}}{r_{e,\,1700\,K\text{ driver}}} = \frac{1700}{900}\left(\frac{2500}{1700}\right)^{-0.6} = 1.50 \tag{4}$$

However, as mentioned, Marklund and Lake observed no difference in erosive rates in the two cases. This observed lack of dependence of the erosive burning rate on core gas temperature tends to cast doubt on all models in the first category of Table 2.

The second category of models listed in Table 2 includes models based upon the alteration of transport properties in the region between the gas flame and the propellant surface by the crossflow, generally due to turbulence effects. Included in this category are models in which the thermal conductivity in this region is raised by turbulence and models in which time for consumption of fuel gas pockets leaving the surface is reduced by the effects of turbulence on diffusivity. Four of these models were developed for double-base propellants as indicated, and will not be reviewed here. Of the compositve propellant models in this category, that of Lengelle[17] appears to be the most advanced. The basic propellant combustion mechanism assumed is the granular diffusion model in which pockets of fuel vapor leave the surface and burn away in an oxidizer continuum at a rate strongly dependent upon the rate of micromixing of the oxidizer vapor into the fuel vapor pocket. The driving mechanism by which the crossflow is assumed to increase the burning rate is through increased turbulence associated with increasing crossflow raising the turbulent diffusivity in the mixing region (thus increasing rate of mixing of the binder and oxidizer product gases) and raising the effective turbulent thermal conductivity. The increase in thermal conductivity increases the heat transfer rate from the flame to the surface, while the increase in mixing rate just offsets the increase in gas velocity away from the surface, with the result that the flame offset distance remains constant. There are several weaknesses associated with the Lengelle model: 1) the granular diffusion flame model is not physically realistic; 2) the ammonium perchlorate monopropellant flame is ignored; and 3) the boundary-layer treatment used to calculate the dependence of the effective turbulent diffusivity and conductivity on the crossflow is unrealistic in its use of a 1/7th power velocity law all the way from the freestream to the surface.

Of the three models listed in the third category (models based on chemically reacting boundary-layer theory) one is complete, while the remaining two are in development. The completed model, by Tsuji,[22] is unfortunately not particularly useful due to the assumption of a totally laminar boundary layer and limitation to a situation where the freestream velocity is proportional to the distance from the head end of the grain. Other simplifications include assumption of premixed stoichiometric fuel and oxidizer (rendering the model inapplicable to compositve propellant systems) and use of one-step global kinetics.

In the model of Beddini et al.[23] primary emphasis is placed on analysis of a well-developed turbulent flowfield in a propellant grain port for definition of turbulent transport of heat, mass, and momentum in the boundary layer. An extended version of the second-order closure method of Donaldson is used to calculate the details of the turbulent flowfield. To date, this flowfield analysis has been coupled only with a simple model of propellant combustion in which the mass burning rate is assumed to be directly proportional to the heat flux from the gas to the surface, and the gas phase reaction is assumed to be described as a single-step homogeneous reaction, with no consideration of the heterogeneity of flame structure associated with composite propellants.

Kuo and Razdan[24] are also using a second-order turbulence closure model for characterization of the flowfield in erosive burning situations, the closure model being used differing from that being used by Beddini. In addition, postulated flame mechanisms (the details of which are unknown to this author) for composite propellants are being coupled into the analysis. At this time, the governing equations have been developed and boundary conditions defined, but the equation solving procedure has not been completed.

The Klimov model[25] is mainly aimed at calculation of threshold crossflow velocities (below which the propellant is unaffected by crossflow). Klimov claims that the threshold velocity is the mainstream crossflow velocity above which the "turbulence front" subsides onto the propellant surface, and presents boundary-layer analysis procedures for calculating this threshold velocity as a function of the transpiration (blowing) velocity of the gases ablating from the propellant surface. In addition, he postulates that negative erosion (sometimes seen at low crossflow velocities) is due to the "stirring up" of cool streams of binder decomposition products over the oxidizer surface, leading to intensification of their cooling effect and to screening of heat feedback from the diffusion flame.

Molnar's model,[26] developed for homogeneous propellants with a laminar crossflow, is based on an assumption (which does not appear to this author to be substantiated) that the lateral velocity gradient at the burning surface governs erosive burning. Miller[27] assumes that the time for a unit of propellant to be consumed is a linear sum of a chemical

reaction time and "the time required for turbulent transport of heat to the propellant surface;" such an addivitity approach does not appear to this author to be physically realistic.

Of the models briefly discussed above, those of Lengelle,[17] Beddini et al.,[23] and Kuo and Razdan[24] appear to be the most advanced (although it is not clear at this time how the latter two teams will build the complex heterogeneous flame structure associated with composite propellant combustion into their fluid dynamic boundary-layer treatments). Common to all three of these models is the assumption that the increase in propellant burning rate associated with crossflow results from turbulence associated with this crossflow penetrating between the propellant gas flame zone(s) and the surface. This turbulence causes increases in mass and energy transport rates. However, for a typical propellant containing oxidizer particles with diameters of from 10 to 50 μm, diffusion flame offset distances may be calculated to be typically of the order of one-quarter to one-half of the particle diameter or 2.5 to 25 μm. On the other hand, for a crossflow velocity of 200 m/s (650 ft/s), the universal u^+, y^+ correlation (transpiration effects neglected) indicates a laminar sublayer thickness of approximately 10 μm and a buffer zone of approximately 50 μm, full turbulence not being achieved closer than 60 μm from the propellant surface. Moreover, transpiration of the binder and oxidizer decomposition gases from the propellant surface will tend to increase the thickness of these zones. Thus it is not at all certain that crossflow-induced turbulence penetrates into the zone between the propellant surface and the gas-phase flame zone(s). In addition, even if the turbulent region does extend into this zone, in order for the eddies to have significant effect on mixing, and thus on heat and mass transfer, they must be considerably smaller than the flame offset distance—that is, they must be on the order of 1 μm in diameter or less. It is not at all clear to this author that a significant degree of turbulence of this scale will be induced in the zone between the propellant surface and the gas-phase flame zone(s) by crossflows even up to Mach 1, more than an order of magnitude above typical erosive burning threshold velocities. Accordingly, an alternate possible mechanism for erosive burning of composite propellants is presented below.

It should be emphasized that this author is not claiming that turbulence effects on mixing and heat transfer do not contribute to erosive burning; in fact, in low-pressure regimes where the combustion layers are quite thick and in homogeneous propellants where there is an induction region of appreciable thickness, this is probably an important mechanism. The attempt here, however, is to see whether in regimes where columnar diffusion flames are important and overall flame heights are possibly less than laminar sublayer thicknesses, the alternative mechanism of flame bending will yield predicted erosive burning rates in reasonable agreement with measurements. It has been argued that use of the classic logarithmic-velocity profile law is inconsistent with dismissal of turbulence as a cause of erosive burning through its effect on heat and mass transfer. However, the u^+, y^+ correlation does include, as discussed above, a laminar sublayer region of appreciable thickness in comparison with estimated flame thicknesses. In addition, even if turbulence does affect heat and mass transfer through increases in eddy conductivity and diffusivity by penetration inside the flame regions, these effects may be negligibly small compared to flame-bending effects unless the diffusion flame extends well past the laminar sublayer and buffer zone into the fully turbulent part of the boundary layer.

Model Development

In development of a proper model of composite propellant erosive burning, it is necessary that a physico-chemical mechanism for the "normal" (no crossflow) burning of such propellants be specified, that the boundary-layer flow be properly described (theoretically or empirically), and that the descriptions of these processes be properly coupled.

Considering first the flowfield, it is informative to estimate flow profiles and angles near the surface of a composite propellant for a typical erosive burning situation. As an example, let us examine a case where the operating pressure is 6.89 (10^6) N/m^2 (1000 psi), the propellant flame temperature is 3000 K, the crossflow mainstream velocity is 200 m/s (650 ft/s), the characteristic length dimension for determining Reynold's number is 15 cm (0.5 ft), and the propellant burning rate is 1.25 cm/s (0.5 in./s). In this case, the gas velocity away from the surface at the flame temperature is approximately 4 m/s (13 ft/s). Using Mickley and Davis[29] flow-profile data for boundary-layer profiles in the presence of transpiration, we estimate that the crossflow velocity 10 μm from the propellant surface is about 10 m/s (30 ft/s). A simplified energy balance equating heat feedback flux from a flame sheet above a propellant surface to the value required for preheating and vaporizing the solid ingredients at a regression rate of 1.25 cm/s (0.5 in./s) indicates that the gas-phase flame must be on the order of 10 μm from the surface. Thus, at the position of the gas-phase flame front, the velocity component away from the propellant is about 4 m/s, while the velocity component parallel to the surface is 10 m/s, and the resultant flow vector makes an angle with the propellant surface of only 22 deg. While this vector will vary with distance from the surface (since the velocity components normal to and parallel to the surface do not scale with distance from the surface in exactly the same way) the variation will not be great. Thus fuel and oxidizer gas columns leaving the surface will not flow perpendicular to the surface (as they would in the absence of crossflow) but at an angle of approximately 20-25 deg from parallel with the surface.

The important feature of this picture is that any diffusion flame at the AP-binder boundaries is bent over toward the propellant surface by the crossflow velocity. Since the deflection of this mixing column or cone can be shown to cause the distance from the base to the tip, measured perpendicular to the base, to decrease, the height above the propellant at which any given fraction of the mixing of AP products and fuel decomposition products is complete should, therefore, be decreased and the distance from the propellant surface to the "average" location of the diffusion flame should also be decreased. This, in turn, will increase heat feedback and thus increase burning rate. The schematic of a

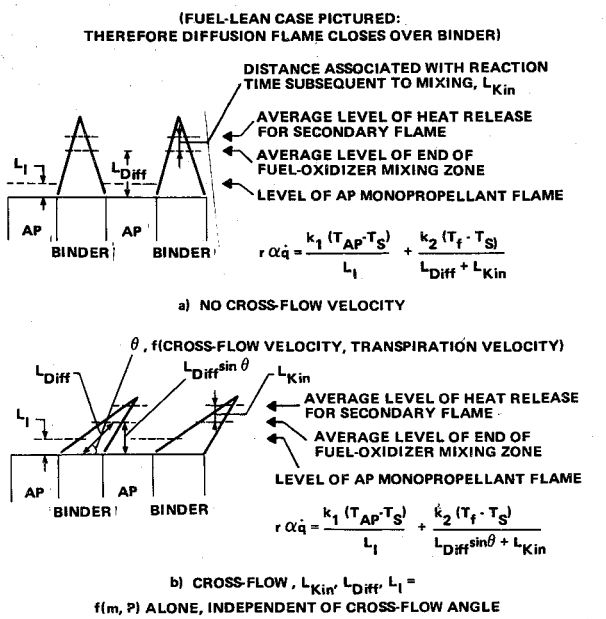

Fig. 1 Schematic of geometrical model of erosive burning (two-flame model).

composite propellant erosive burning model based upon this picture is shown in Fig. 1.

In the first part of the figure, the flame processes occurring in the absence of crossflow are depicted. There are two flames considered, an ammonium perchlorate deflagration monopropellant flame close to the surface and a columnar diffusion flame resulting from mixing and combustion of the AP deflagration products and fuel-binder pyrolysis products at an average distance somewhat further from the surface. Three important distance parameters considered are the distance from the propellant surface to the "average" location of the kinetically controlled AP monopropellant heat release (L_1), the distance associated with mixing of the oxidizer and fuel for the diffusion flame (L_{diff}), and the distance associated with the fuel-oxidizer reaction time subsequent to mixing (L_{kin}). A heat balance between heat feedback from these two flames and the energy requirements for heating the propellant from its initial temperature to the burning surface temperature and then decomposing it yields (assuming that the heat feedback required per unit mass of propellant consumed is independent of burning rate)

$$r \propto \dot{q}_{\text{feedback}} \propto \frac{k_1 (T_{\text{AP}} - T_s)}{L_1} + \frac{k_2 (T_f - T_s)}{L_{\text{diff}} + L_{\text{kin}}} \tag{5}$$

The method of summing heat fluxes from the two different flame zones with use of constants k_1 and k_2 that include not only thermal conductivities but also fractions of total surface area over which each flame contributes importantly is somewhat arbitrary in that these fractions are thus assumed to be independent of burning rate. However, it is felt that this assumption should not produce gross errors and relaxation of this assumption with detailed calculation of superposition of the fluxes destroys the simplicity of the model. A second-generation model in which this assumption is relaxed is currently under development.

The situation pictured as prevailing with a crossflow is shown in the second part of Fig. 1. Since L_1 and L_{kin} are both kinetically controlled, and are thus simply proportional to a characteristic reaction time (which is assumed to be unaffected by the crossflow) multiplied by the propellant gas velocity normal to the surface (which for a given formulation is fixed by burning rate and pressure alone), these distances are fixed for a given formulation at a given burning rate and pressure, independent of the crossflow velocity. Of course, since crossflow velocity affects burning rate at a given pressure through its influence on the diffusion process as discussed below, L_1 and L_{kin} are influenced through the change in burning rate. This is simply coupled into a model by expressing L_1 and L_{kin} as explicit functions of burning rate and pressure in that model. The important point is that they can be expressed as functions of only these two parameters for a given propellant. However, the distance of the mixing zone from the propellant surface is directly affected by the crossflow. It may be shown through geometrical arguments coupled with the columnar diffusion flame-height analysis presented by Schultz et al.,[5] that L_{diff} measured along a vector coincident with the resultant crossflow and transpiration velocities should be approximately the same as L_{diff} in the absence of a crossflow at the same burning rate and pressure (except at very high ratios of local crossflow velocity to transpiration velocity). That is, the magnitude of L_{diff} is essentially independent of the crossflow velocity, although its orientation is not. Thus, the distance from the surface to the "average" mixed region is decreased to $L_{\text{diff}} \sin\theta$ where θ represents the angle between the surface and the average flow vector in the mixing region. The heat balance at the propellant surface now yields

$$r \propto \dot{q}_{\text{feedback}} \propto \frac{k_1 (T_{\text{AP}} - T_s)}{L_1} + \frac{k_2 (T_f - T_s)}{L_{\text{diff}} \sin\theta + L_{\text{kin}}} \tag{6}$$

This picture has been used as the basis of development of a model for prediction of burning rate vs pressure curves at various crossflow velocities, given only a curve of burning rate vs pressure in the absence of crossflow. This model employs no empirical constants other than those obtained from regression analysis of the no-crossflow burning rate data. Therefore, although it is not as powerful as a model that permits prediction of erosive burning phenomena with no burning rate data at all, but only propellant composition and ingredient size data, it is still a very useful tool because it permits prediction of erosive burning characteristics given only relatively easily obtained strand-bomb burning rate data. (By comparison, the Lenoir and Robillard model employs two free constants which are adjusted to provide a best fit of erosive burning data for a given propellant. Since these constants vary from propellant to propellant, the Lenoir and Robillard model does not permit a priori erosive burning predictions for new propellants without some erosive burning data, whereas the model presented here does not require such data.)

The general approach followed in development of this model is as follows:

1) The expressions for L_1, L_{diff}, and L_{kin} as functions of burning rate (or burning mass flux $\dot{m}$), pressure, and propellant properties are derived and substituted into a propellant surface heat balance.

2) The resulting equation is worked into the form of Eq. (12) (developed in succeeding paragraphs) for burning in the absence of crossflow. A regression analysis using no-crossflow burning rate data is performed to obtain best fit values for A_3, A_4 and A_5, three constants appearing in this expression. (d_p is the average ammonium perchlorate particle size. For a given propellant, the burning rate data may be just as effectively regressed on A_3, A_4, and $A_5 d_p^2$, eliminating the necessity of actually defining an effective average particle size.)

3) From these results, expressions are obtained for L_1, L_{diff}, and L_{kin} as functions of burning rate (or $\dot{m}$) and pressure.

4) These expressions are combined with analysis of the boundary-layer flow (which gives the crossflow velocity as a function of distance from the propellant surface, mainstream velocity, and propellant burning rate) to permit calculation of the angle θ (Fig. 1), L_1, L_{diff}, L_{kin}, and $\dot{m}$ for a given pressure and crossflow velocity.

In the derivation of a burning rate expression for a composite propellant in the absence of a crossflow, an energy balance at the propellant surface is first written as (see Fig. 1).

$$\frac{\lambda_A (T_f - T_s)}{(L_{\text{diff}}) + (L_{\text{kin}})} + \frac{\lambda_B (T_{\text{AP}} - T_s)}{L_1} = \dot{m} [c_p (T_s - T_0) + Q_{\text{VAP}} - Q_{RX}] \tag{7}$$

The first term of this equation represents heat flux from the final flame to the surface; the second represents heat flux from the AP monopropellant flame; and the third represents the heat flux requirements for ablation of the propellant at the mass flux, $\dot{m}$. Several simplifying assumptions are obviously involved in writing of the equation in this form. Probably the most important and tenuous of these is the assumption that Q_{RX} is independent of burning rate (or $\dot{m}$) and of pressure. In the Zeldovich picture of solid-propellant combustion, where subsurface exothermic reactions with fairly high activation energies are considered to dominate, this would be a very poor assumption. However, in the generally accepted picture of solid-propellant combustion in this country, it is not a bad approximation. In addition, it is assumed that the surface temperature is nearly constant with respect to pressure and burning rate, with the resultant uncoupling of this heat balance equation from a surface regression rate Arrenhius expression. Finally, it is assumed that for the diffusion flame,

a distance associated with mixing may be added linearly to a distance associated with reaction delay to yield a total flame offset distance. This description is oversimplified.

The monopropellant AP flame offset distance, L_1, may be expressed as the product of a characteristic reaction time, τ_1, and the linear velocity of gases leaving the propellant surface

$$L_1 = \tau_1 \frac{\dot{m}}{\rho_{\text{gas}}} \tag{8}$$

For a second-order gas-phase reaction (generally assumed), τ_1 is inversely proportional to pressure, and for a given formulation, the gas density is directly proportional to pressure, yielding

$$L_1 = K_1 \dot{m}/P^2 \tag{9}$$

A similar analysis for L_{kin} yields

$$L_{\text{kin}} = K_2 \dot{m}/P^2 \tag{10}$$

For a columnar diffusion flame, it may easily be shown[30] that the diffusion cone height, L_{diff}, may be expressed as

$$L_{\text{diff}} = K_3 \dot{m} d_p^2 \tag{11}$$

Equations (7) and (9-11) may be combined to yield

$$r = \dot{m}/\rho_s = A_3 P[1 + A_4/(1 + A_5 d_p^2 P^2)]^{1/2} \tag{12}$$

Burning rate vs pressure data for a given propellant in the absence of a crossflow may then be analyzed via a fairly complicated regression analysis procedure to yield values of the constants A_3, A_4, and A_5 (or $A_5 d_p^2$) for that given propellant. The constants K_1, K_2, and K_3 are related to these constants in turn by

$$K_1 = (T_{\text{AP}} - T_s)\lambda_B / A_2 A_3^2 \lambda_A \tag{13}$$

$$K_2 = (T_f - T_s)/A_2 A_3^2 A_4 \tag{14}$$

$$K_3 = (T_f - T_s) A_5 / A_2 A_3^2 A_4 \tag{15}$$

where

$$A_2 = \frac{\rho_s^2 [c_p (T_s - T_0) + Q_{\text{VAP}} - Q_{RX}]}{\lambda_A} \tag{16}$$

In this analysis a rough estimate of A_2 has been made to permit calculation of values of K_1, K_2, and K_3 from the best-fit values of A_3, A_4, and A_5. It should be pointed out, however, that the subsequent calculations of burning rates in crossflows are not strongly affected by the estimate of A_2, since the same value of A_2 is used in that analysis, and thus its effects essentially cancel. The value used for most cases (except those cases run to test the effect of A_2) was 2×10^6 g-s-K/cm^5.

Data of Mickley and Davis[29] were used to develop empirical expressions for the local crossflow velocity as a function of distance from the propellant surface, mainstream crossflow velocity, and transpiration rate (gas velocity normal to the propellant surface). In this analysis, it was decided that the transpiration velocity should be calculated as the gas velocity normal to the surface at the final flame temperature. (Mickley and Davis correlations are based upon the ratio of mainstream velocity to transpiration velocity.) The procedure used is outlined in Table 3.

The above analyses were used in the derivation of the following eight equations in eight unknowns for the burning of a given composite propellant at a given pressure and

Table 3 Calculation of crossflow velocity profile in current erosive burning model

1) Neglecting transpiration effects

Calculate $U^* = U_{\text{mainstream}} \sqrt{\frac{f}{2}} = \frac{0.152 U_{\text{mainstream}}}{(Re)^{0.1}}$

$$= \frac{0.023 (U_{\text{mainstream}}^{0.9})(273 + T_f)^{0.18}}{D^{0.1} p^{0.1}}$$

Calculate $Y^+ = YU^*\rho/u$

Calculate $U^+ = Y^+$ for $Y^+ < 5$

$U^+ = -3.05 + 5.00 \ln Y^+$ for $5 < Y^+ < 30$

$U^+ = 5.5 + 2.5 \ln Y^+$ for $Y^+ > 30$

Calculate $U = U^+ U^*$

2) Allowing for transpiration (using data of Mickley and Davis) do all of the above and correct result by

$$U_{\text{transpiration case}} = U_{\text{no transpiration}} \exp(-60\, V_{\text{transpiration}}/U_{\text{mainstream}})$$

crossflow velocity:

$$r = \frac{K_2'}{L_{\text{diff}} \sin\theta + L_{\text{kin}}} + \frac{K_7'}{L_1} \tag{17}$$

$$L_{\text{diff}} = K_1' r \tag{18}$$

$$L_{\text{kin}} = K_5' r \tag{19}$$

$$L_1 = K_6' r \tag{20}$$

$$V_{\text{transpiration}} = K_3' r \tag{21}$$

$$Y^+_{y = L_{\text{diff}} \sin\theta} = K_8' r \sin\theta \tag{22}$$

$$U_{\text{crossflow}, y = L_{\text{diff}} \sin\theta} = K_9' f(Y_{y = L_{\text{diff}} \sin\theta}^+) \tag{23}$$

$$\sin\theta = \frac{V_{\text{transpiration}}}{\sqrt{V_{\text{transpiration}}^2 + U_{\text{crossflow}, y = L_{\text{diff}} \sin\theta}^2}} \tag{24}$$

where

$$K_1' = \frac{(T_f - T_s) A_5 d_p^2 \rho_s}{A_2 A_3^2 A_4} \tag{25}$$

$$K_2' = \rho_s (T_f - T_s)/A_2 \tag{26}$$

$$K_3' = RT_f \rho_s / P(MW) \tag{27}$$

$$K_5' = (T_f - T_s)\rho_s / A_2 A_3^2 A_4 P^2 \tag{28}$$

$$K_6' = (T_{\text{AP}} - T_s)\rho_s \lambda_B / A_2 A_3^2 P^2 \lambda_A \tag{29}$$

$$K_7' = [\rho_s (T_{\text{AP}} - T_s)/A_2](\lambda_B/\lambda_A) \tag{30}$$

$$K_8' = \frac{K_1' U^* \rho_{\text{gas}, T = (Tf + Ts)/2}}{\mu_{\text{gas}, T = (T_f + T_s)/2}} \quad \text{(see Table 3)} \tag{31}$$

$$K_9' = U^* \quad \text{(see Table 3)} \tag{32}$$

and the function f of Eq. (23) is given in Table 3.

Implicit in Eq. (24) is the assumption that the transpiration velocity and the crossflow velocity maintain a constant ratio from very near the surface out to the end of the diffusion zone; that is, that the vector resultant is a straight line. This approximation is reasonably accurate and should not strongly affect the results of the calculations.

As may be seen, the quantity A_2 appears in the denominator of K_2', K_7', K_1', K_5' and K_6'. Thus, as indicated earlier, the effect of A_2 in Eq. (17) cancels out and the predicted burning rate is dependent upon this parameter only to the extent that it affects the calculation of the crossflow velocity at distance $L_{\text{diff}} \sin\theta$ from the surface. Parametric calculations with various values of A_2 indicate that this effect is very weak. A computer code has been developed to solve these equations simultaneously, yielding a predicted burning rate for a given pressure, crossflow velocity, and sets of constants A_3, A_4, and $A_5 d_p^2$ obtained from regression analysis of no-crossflow data.

Comparison of Predictions with Data

Original testing of the model was carried out using a systematic erosive burning data set taken by Saderholm. (This was the only systematic data found in the literature with sufficient zero crossflow data to permit evaluation of A_3, A_4, and $A_5 d_p^2$.) The computer code described above was used to calculate burning rate vs pressure curves for several crossflow velocities studied by Saderholm, with and without correction of the boundary-layer profiles for transpiration effects. The results are shown in Figs. 2 and 3. As shown in Fig. 2, neglecting correction for the effects of transpiration on the boundary-layer profile results in serious overprediction of the burning rates. However, as shown in Fig. 3, agreement between predictions and data is excellent when the transpiration correction factor is included.

In parallel with this modeling effort, Atlantic Research is carrying out an experimental test program to obtain systematic erosive burning data for a series of propellant formulations. This experimental program is described in some detail in Ref. 1 and 31. At this time, a fairly complete set of data covering a pressure range of $1\text{-}5\times10^6$ n/m^2 (10 to 50 atm and a crossflow velocity range of 200 to 700 m/s (600 to 2200 ft/s) has been obtained for one formulation, designated Formulation 4525. This is a "scholastic" formulation, containing unimodal ammounium perchlorate. The formulation consists of 73 wt% 20-μm diameter ammonium perchlorate (AP) and 27 wt% hydroxyterminated polybutadiene (HTPB) binder, with a trace of carbon black added to opacify the propellant. Experimental and theoretical results are presented in Figs. 4 and 5. As may be seen, agreement between prediction and data, while not as good as with the Saderholm propellant, is nevertheless valid. The predicted curves for burning rate vs pressure at various crossflow velocities (Fig. 4) do seem to group more tightly than the data. That is, as shown more clearly in Fig. 5, the model tends to overpredict the burning rate at low crossflow velocities and underpredict it at high velocities.

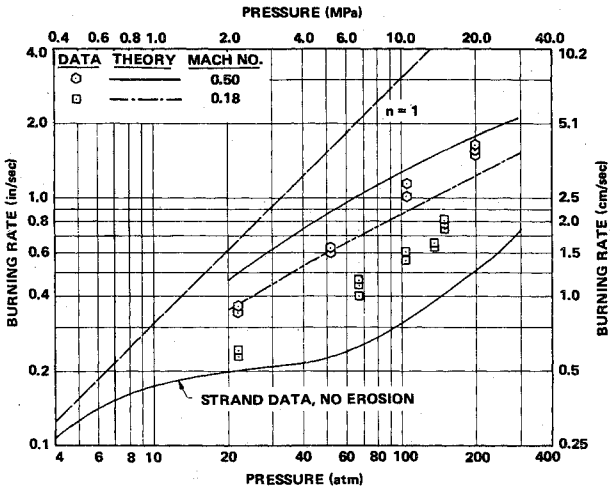

Fig. 2 Erosive burning model predictions and comparisons with Saderholm data. Transpiration effects not included.

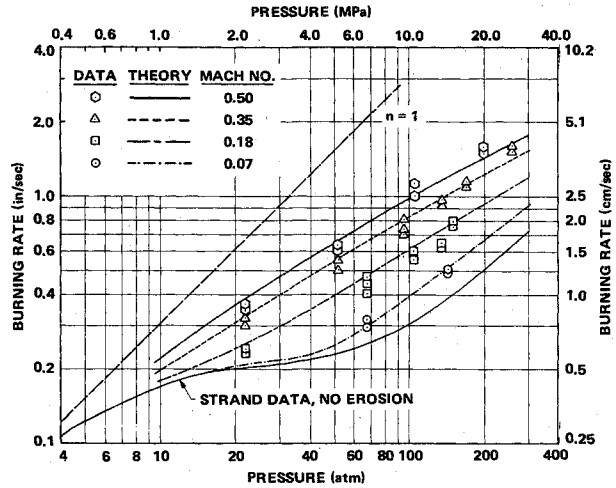

Fig. 3 Erosive burning model predictions and comparisons with Saderholm data. Transpiration effects included.

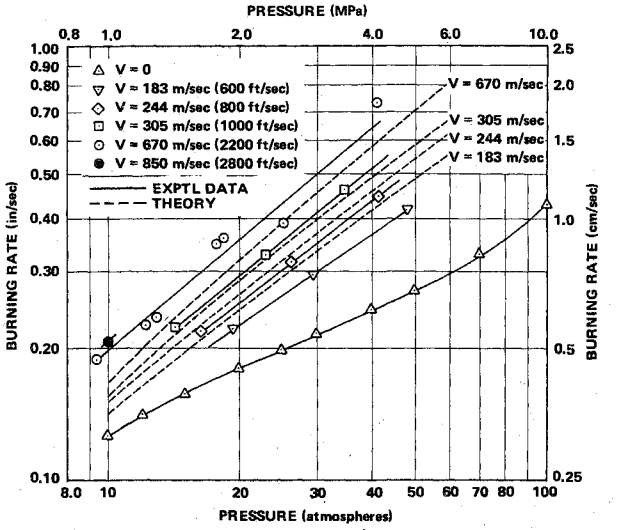

Fig. 4 Burning rate vs pressure data and predictions for various crossflow velocities for Formulation 4525 (73/27 AP/HTPB, 20 μm AP).

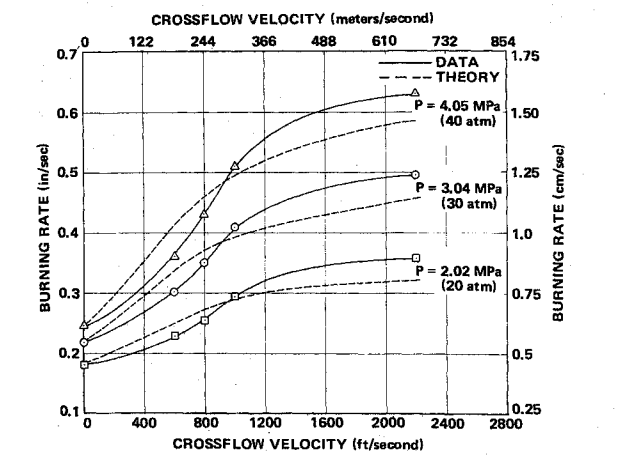

Fig. 5 Burning-rate vs crossflow data and predictions for various pressures for Formulation 4525 (73/27 AP/HTPB, 20 μm AP).

Summary

Past modeling efforts in the area of erosive burning of solid propellants have been reviewed, and lack of a model which incorporates a realistic description of composite propellant combustion has been noted. A possible physical mechanism by which crossflows may affect the combustion of a composite propellant has been postulated and a mathematical model for prediction of the burning rate of a composite propellant in such a crossflow, given only the no-crossflow burning rate vs pressure characteristics of the propellant, has been developed. This model has been used to predict remarkably well the erosive burning characteristics of a propellant studied by Saderholm. In addition, reasonable agreement between predictions and data has been obtained for a formulation recently characterized in our test facility. Additional propellants are currently being studied, and erosive burning rate data and predictions for these formulations will be compared for further testing of the model in the near future. In addition, a second-generation model based on this same picture, which does not require no-crossflow burning rate vs pressure data but instead uses only propellant composition and ingredient size as input, is currently under development.

Acknowledgment

This effort was supported by AFOSR under Contract No. F44620-76-C-0023, monitored by T. Meier.

References

[1] King, M.K., "Effects of Crossflow on Solid Propellant Combustion: Interior Ballistic Design Implications," 1976 JANNAF Propulsion Meeting, Atlanta, Ga.,Dec. 1976, CPIA Publication 280, Vol. V., p. 431.

[2] Viles, J.M., "Prediction of Rocket-Motor Chamber Pressures Using Measured Erosive-Burning Rates," Rohm and Haas Co., Huntsville, Ala., Technical Report S-275 (Contract DAAHO1-70-C-0152, Oct. 1970.

[3] Saderholm, C.A., "A Characterization of Erosive Burning for Composite H-Series Propellants," AIAA Solid Propellant Rocket Conference, Palo Alto, Calif., Jan. 29, 1964.

[4] Kriedler, J.W., "Erosive Burning: New Experimental Techniques and Methods of Analysis," AIAA Solid Propellant Rocket Conference, Palo Alto, Calif., Jan. 29, 1964.

[5] Schultz, R., Green, L., and Penner, S.S., "Studies of the Decomposition Mechanism, Erosive Burning, Sonance and Resonance for Solid Composite Propellant," *Combustion and Propulsion,* 3rd AGARD Colloquium, Pergamon, New York, 1958.

[6] Green, L., "Erosive Burning of Some Composite Solid Propellants," *Jet Propulsion,* Vol. 24, Jan.-Feb. 1954, p. 9.

[7] Peretz, A., "Experimental Investigation of the Erosive Burning of Solid Propellant Grains with Variable Port Area," *AIAA Journal,* Vol. 6, May 1968, p. 910.

[8] Marklund, T. and Lake, A., "Experimental Investigation of Propellant Erosion," *ARS Journal,* Vol. 30, Feb. 1960, p. 173.

[9] Dickinson, L.A., Jackson, F., and Odgers, A.L. , "Erosive Burning of Polyurethane Propellants in Rocket Engines," *Eighth Symposium (International) on Combustion,* Williams and Wilkins, Baltimore, 1962, p. 754.

[10] Zucrow, M.J., Osborn, J.R., and Murphy, J.M.,"An Experimental Investigation of the Erosivie Burning Characteristics of a Nonhomogeneous Solid Propellant," *AIAA Journal,* Vol. 3, March 1965, p. 523.

[11] Vilyunov, V.N., Dvoryashin, A.A., Margolin, A.D., Ordzhonikidze, S.K., and Pokhil, P.F., "Burning of Ballistite Type H in Sonic Flow," *Fizika Goreniya i Vzryva,* Vol. 8, Oct. 1972, pp. 501-505.

[12] Lenoir, J.M. and Robillard, G., "A Mathematical Method to Predict the Effects of Erosive Burning in Solid-Propellant Rockets," *Sixth Symposium (International) on Combustion,* Reinhold, New York, 1957, p. 663.

[13] Burick, R.J. and Osborn, J.R., "Erosive Combustion of Double-Base Solid Rocket Propellants," 4th ICRPG Combustion Conference, CPIA Publication 162, Vol. II, Dec. 1967, pp. 57-69.

[14] Zucrow, M.J., Osborn, J.R. and Murphy, J.M., "The Erosive Burning of a Nonhomogeneous Solid Propellant," AICHE Symposium Series No. 52, 1964, pp. 23-29.

[15] Jojic, B. and Blagojevic, D.J., "Theoretical Prediction of Erosive Burning Characteristics of Solid Rocket Propellant Based on Burning Rate Dependence of Pressure and Initial Temperature and its Energetic Characteristics," AIAA Paper 76-697, AIAA/SAE 12th Propulsion Conference, Palo Alto, Calif., July 1976.

[16] Saderholm, C.A., Biddle, R.A., Caveny, L.H., and Summerfield, M., "Combustion Mechanisms of Fuel Rich Propellants in Flow Fields," AIAA Paper No. 72-1145, AIAA/SAE 8th Joint Propulsion Specialist Conference, New Orleans, La., Nov. 29, 1972.

[17] Lengelle, G., "Model Describing the Erosive Combustion and Velocity Response of Composite Propellants," *AIAA Journal,* Vol. 13, March 1975, pp. 315-322.

[18] Corner, J., *Theory of the Interior Ballistics of Guns,* Wiley, New York, 1950.

[19] Vanderkerckhove, J., "Erosive Burning of a Colloidal Solid Propellant," *Jet Propulsion,* Vol. 28, Sept. 1958, pp. 599.

[20] Zeldovich, Y.B., "Theory of Propellant Combustion in a Gas Flow," *Fizika Goreniya i Vzryva,* Vol. 7, Oct. 1971, pp. 463-376.

[21] Geckler, R.E. et al., Aerojet Engineering Corporation, Report 445, 1950.

[22] Tsuji, H., "An Aerothermochemical Analysis of Erosive Burning of Solid Propellant," *Ninth International Symposium on Combustion,* Academic Press, New York, 1963, pp. 384-393.

[23] Beddini, R.A. and Fishburne, E.S., "Analysis of the Combustion-Turbulence Interaction Effects on Solid Propellant Erosive Burning," AIAA Paper 77-931, AIAA 13th Propulsion Conference, Orlando, Fla., July 1977.

[24] Kuo, K.K., Razdan, M.K., and Kovalcin, R.L., "Theoretical and Experimental Investigation of Erosive Burning of Non-Metalized Composite Solid Propellants," presented at 1977 Joint AFOSR/AFRPL Rocket Propulsion Research Meeting, Lancaster, Calif., March 1977.

[25] Kilmov, A.M., "Erosive Burning of Propellants," *Combustion, Explosion and Shock Waves,* Vol. 11, Oct. 1976, p. 678.

[26] Molnar, O., "Erosive Burning of Propellant Slabs," AIAA Paper 72-1108, AIAA/SAE 8th Joint Propulsion Specialist Conference, New Orleans, La., Nov. 1972.

[27] Miller, E., "Erosive Burning of Composite Solid Propellants," *Combustion and Flame,* Vol. 10, Dec. 1966, p. 330.

[28] King, M.K., "A Modification of the Composite Propellant Erosive Burning Model of Lenoir and Robillard," *Combustion and Flame,* Vol. 24, June 1975, pp. 365-368.

[29] Mickley, H.S. and Davis, R.S., "Momentum Transfer for Flow Over a Flat Plate with Blowing," NACA Technical Note 4017, Nov. 1957.

[30] Sutherland, S.G., "The Mechanism of Combustion of an Ammonium Perchlorate-Polyester Resin Composite Solid Propellant," Ph.D. Thesis, Princeton University, 1956.

[31] King, M., "Erosive Burning of Composite Propellants," 13th JANNAF Combustion Meeting, Monterey, Calif., Sept. 1976, CPIA Publication 281, Vol. II, p. 407.